# Qualitative Study of a Planar Pursuit Evasion Game in the Atmosphere

M. Guelman*
*Rafael, Ministry of Defense, Haifa, Israel*
and
J. Shinar† and A. Green‡
*Technion—Israel Institute of Technology, Haifa, Israel*

**A coplanar pursuit-evasion game of kind in the atmosphere between a coasting pursuer and a maneuvering evader of constant speed is considered. The aerodynamic forces acting on the pursuer are modeled in two different forms: one for small and the other for large angles of attack. For both models the adjoint equations can be integrated analytically starting at the circular target set of the game. This allows one to determine the optimal strategies of the pursuer and the evader on the boundary of the capture set, called the "barrier." On the barrier the existence of singular surfaces for the evader are observed. A representative example of barrier trajectories starting on the dispersal surface is given.**

## I. Introduction

REALISTIC pursuit evasion games, opposing a missile to a maneuvering aircraft in the atmosphere, are characterized by an inherent dissymmetry. The missile is designed to be faster and more maneuverable than the aircraft. This kinematical advantage is, however, temporary. The rocket motor accelerating the missile to a high velocity is of short duration. In the coasting phase, the high, but finite, kinetic energy of the missile is rapidly dissipated by the work done against the aerodynamic drag. On the other hand, the fuel flow of an aircraft being rather slow allows the aircraft to maintain constant or slowly varying velocity for a very long period of time. This fact can be interpreted as that the evader has in practical terms almost unlimited energy. The basis of the dissymmetry between pursuer and evader is therefore kinematic advantage vs energy conservation advantage. The above outlined dissymmetry results in the temporary nature of the kinematic advantage of the missile (the pursuer). Consequently, the evading aircraft cannot be reached from every initial state.

Analysis of pursuit evasion games between constant speed vehicles[1,2] showed that a faster and more maneuverable pursuer can achieve "point capture" in a finite time from any initial condition. The optimal strategies in such a game, with the time of capture as the payoff,[3] are for both players to turn at maximum rate toward the final line-of-sight direction. Once the players reach this line they continue to move along it until capture. In the game between two variable speed players,[4] the optimal strategies are similar; both players turn toward the final line-of-sight direction with an asymptotically decaying rate and in effect never reach this final direction. The game was analyzed employing a real-space coordinate system whose origin and axes changed from party to party and each player's optimal motion in real space was described in terms of a map of trajectories independent of adversary and role. The game solution was obtained by combining these trajectory maps parameterized by the small but nonzero difference between the final-flight direction and final line of sight.

Received Oct. 25, 1988; revision received May 30, 1989. 

*Deputy Director, Guidance Division.

†Professor, Faculty of Aerospace Engineering. Associate Fellow AIAA.

‡Graduate Student, Faculty of Aerospace Engineering.

In the present paper, the missile vs aircraft encounter is formulated as a qualitative, pursuit-evasion game (game of kind). The objective in solving such a game is to determine the set of initial conditions from which the optimally played game terminates with the victory of the pursuer. In a game of kind, the pursuer wins if the "target set" of the game is reached in some finite time. The target set is defined by some prescribed criterion of "capture" (not necessarily point-capture) depending on the problem. In a game of kind, there is no specific payoff function. The zone of pursuer's victory is called the "capture set" of the game, and the objective of the pursuer is to maximize the zone, while the evader attempts to minimize this zone. The game of kind solution also yields the optimal strategies of the players along the boundary of the capture set. In the context of a missile vs aircraft encounter, the capture set corresponds to the effective (no-escape) firing envelope of the missile.

The simplest model for such a game preserving the salient features of the original problem is of coplanar geometry between a coasting pursuer and a constant-speed evader.

Several versions of such a model were investigated in recent years. In Ref. 5 the attainability domain of a coasting vehicle was studied and in Ref. 6 the capture region of this pursuer opposed to a constant velocity evader in simple motion was analyzed. In both of these works, the aerodynamic forces acting on the pursuer were explicitly defined as functions of the angle of attack. In Ref. 7 the case of a coasting pursuer, using a parabolic drag model and employing proportional navigation opposed to a constant velocity maneuvering evader, was investigated as an optimal evasion problem.

The objective of the present paper is to study the qualitative game solution with the previously described dynamics using suitable aerodynamic models, for both small and large angles of attack.

## II. Problem Definition

The geometry of planar pursuit defining the state variables of the game is depicted in Fig. 1. A vehicle $P$, called the pursuer, possessing a velocity $V_P$ is pursuing in planar motion a second vehicle, the evader $E$, assumed to be flying with a constant velocity $V_E$.

The equations of motion are

$$\dot{R} = V_E \cos(\gamma_E - \theta) - V_P \cos(\gamma_P - \theta) \tag{1}$$

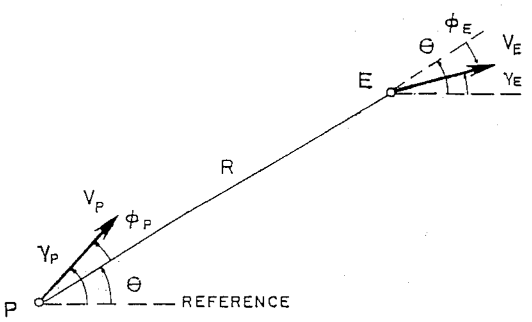


**Fig. 1 Geometry of planar pursuit.**

$$\dot{\theta} = [V_E \sin(\gamma_E - \theta) - V_P \sin(\gamma_P - \theta)]/R \tag{2}$$

$$\dot{\gamma}_E = \Gamma_E u_E \tag{3}$$

$$\dot{V}_P = -k_P V_P^2 C_D \tag{4}$$

$$\dot{\gamma}_P = \Gamma_P u_P \tag{5}$$

where $k_P$ is a constant depending on the altitude, $C_D$ is the nondimensional drag coefficient, $\Gamma_E$ and $\Gamma_P$ are the maximum turning rates of the evader and the pursuer, respectively, and $u_E$ and $u_P$ are the controls.

The $\Gamma_E$ and $\Gamma_P$ depend on the maximum lateral acceleration available to the players and are therefore functions of the flight conditions. For a constant-speed vehicle in horizontal flight, the value of $\Gamma$ is constant.

Neglecting gravity, the turning rate of the pursuer is given by

$$\Gamma_P u_P = k_P V_P C_L \tag{6}$$

where $C_L$ is the nondimensional lift coefficient having a limit value of $C_{L\max}$, i.e.,

$$\Gamma_P = k_P V_P C_{L\max} \tag{7}$$

For the aerodynamic coefficients $C_L$ and $C_D$, two different models are considered. For missiles operating in the domain of small angles of attack, a linear lift

$$C_L = C_{L\alpha}\alpha \tag{8}$$

and a parabolic drag polar

$$C_D = C_{D0} + (KC_{L\alpha}^2)\alpha^2 \tag{9}$$

model are appropriate. For missiles of high maneuverability, requiring large angles of attack, a nonlinear aerodynamic model, used in Refs. 5 and 6, is more representative:

$$k_P C_L = c_1 \sin 2\alpha \tag{10}$$

$$k_P C_D = c_1(k - \cos 2\alpha) \tag{11}$$

The coefficients $c_1$ and $k$ are derived in Appendix A.

Let us define new normalized variables,

$$r \overset{\Delta}{=} R/R_{\text{ref}} \tag{12}$$

$$v \overset{\Delta}{=} V_p/V_E \tag{13}$$

$$t' \overset{\Delta}{=} tV_E/R_{\text{ref}} \tag{14}$$

where $R_{\text{ref}}$ is the minimum admissible turning radius of the pursuer defined by

$$R_{\text{ref}} = V_P/\Gamma_P = 1/[k_P C_{L\max}] \tag{15}$$

Note that for the high-angle-of-attack model, $k_P C_{L\max} = c_1$. With these new variables, and with a dot now denoting the derivative with respect to normalized time $t'$, the pursuit game system of equations for the case of a parabolic drag polar is defined as follows:

$$\dot{r} = \cos(\gamma_E - \theta) - v\cos(\gamma_P - \theta) \tag{16}$$

$$\dot{\theta} = [\sin(\gamma_E - \theta) - v\sin(\gamma_P - \theta)]/r \tag{17}$$

$$\dot{\gamma}_E = \sigma u_E \tag{18}$$

$$\dot{v} = -v^2(a + bu_p^2) \tag{19}$$

$$\dot{\gamma}_P = v u_P \tag{20}$$

where $\sigma$ is the ratio of pursuer's minimum turning radius to that of the evader (in general $\sigma < 1$), $a = C_{D0}/C_{L\max}$ and $b = KC_{L\max}$.

For the nonlinear areodynamic model, Eqs. (19) and (20) become

$$\dot{v} = -(k - \cos 2\alpha)v^2 \tag{21}$$

$$\dot{\gamma}_P = v \sin 2\alpha \tag{22}$$

and $\alpha$ can be used as a control of the pursuer.

This is a fifth-order system. The number of independent variables can be reduced to four, which is the minimal representation of the system, if use is made of the evader and pursuer relative angles with respect to the line of sight, $\phi_E = (\gamma_E - \theta)$ and $\phi_P = (\gamma_P - \theta)$, respectively. However, the use of the reduced system complicates unnecessarily the analysis without any particular advantage. Therefore, in the sequel, Eqs. (16-20) will be employed. The controls of the players are $u_E$ and $u_P$ (or $\alpha$), respectively.

The game described by the preceding equations terminates with capture when the pursuer approaches the evader to a prescribed normalized distance $r_f$. In other words, the target set $T$ of the game is defined as a closed circular cylinder of radius $r_f$:

$$T = \{x \epsilon E^5 : r \le r_f\} \tag{23}$$

where $\boldsymbol{x} = (r, \theta, \gamma_E, v, \gamma_P)^T$ is the state vector, and no additional conditions are imposed on $\theta$, $\gamma_E$, $v$, and $\gamma_P$.

## III. Derivation of Optimal Strategies

The solution of a qualitative game, such as the one formulated in the previous section of this paper, is to determine the boundary of the capture set in the game and the respective optimal strategies. The capture set is the set of all admissible initial conditions $\boldsymbol{x}_0 = (r_0, \theta_0, \gamma_{E0}, v_0, \gamma_{P0})$ from which the pursuer can drive the game to the target set $T$ given in Eq. (23) against any admissible control action of the evader.

The capture set of the present game is a bounded region in the five-dimensional state space. The boundary of the capture set consists of the target set $T$, the hyperplane $v = v_0$ (determined by the initial kinetic energy of the pursuer), and a closed semipermeable hypersurface called the barrier. The barrier is formed by an infinite set of game trajectories [solutions of Eqs. (16-20)] generated by using a pair of optimal strategies $E^*(\boldsymbol{x})$ and $P^*(\boldsymbol{x})$ such that

$$u_E^*(t') = E^*[\boldsymbol{x}(t')] \tag{24}$$

$$u_P^*(t') = P^*[\boldsymbol{x}(t')] \tag{25a}$$

or (for the high-angle-of-attack aerodynamics)

$$\alpha^*(t') = P^*[x(t')] \tag{25b}$$

If the evader employs its optimal barrier strategy $E^*$, then it is guaranteed that the state of the game cannot be driven by any maneuver of the pursuer from the barrier into the interior of the capture set. On the other hand, the pursuer optimal strategy guarantees to deny any attempt of the evader to drive the state of the game to the zone strictly exterior to the capture set. The optimal strategy pair and the respective control actions in Eqs. (24) and (25) can be determined by the min-max principle of qualitative games[8]

$$\min_{u_P} \mathrm{H}(x,p,u_P,u_E^*) = \max_{u_E} H(x,p,u_P^*,u_E) = H(x,p,u_P^*,u_E^*) = 0 \tag{26}$$

where $H(x,p,u_P,u_E)$ is the Hamiltonian of the qualitative game and is defined as the scalar product of the state velocity $x$ and the adjoint vector $p = (p_r, p_\theta, p_{\gamma E}, p_v, p_{\gamma P})^T$.

The vector $p$ represents the gradient of the barrier hypersurface, whenever such a gradient exists. For the present game,

$$H = p_r[\cos(\gamma_E - \theta) - v\cos(\gamma_P - \theta)] + p_\theta[\sin(\gamma_E - \theta) - v\sin(\gamma_P - \theta)]/r + p_{\gamma E}\sigma u_E + H_P \tag{27}$$

with $H_P$ expressed differently for the two aerodynamic models. For small angles of attack,

$$H_P = -p_v v^2(a + bu_p^2) + p_{\gamma P} v u_P \tag{28a}$$

and for the large-angle-of-attack model,

$$H_P = -p_v(k - \cos 2\alpha)v^2 + p_{\gamma P} v \sin 2\alpha \tag{28b}$$

The components of the adjoint vector $p$ have to satisfy the following set of differential equations and transversality conditions:

$$\dot p_r = p_\theta[\sin(\gamma_E - \theta) - v\sin(\gamma_P - \theta)]/r^2, \quad p_{rf} = \mu, \quad \mu > 0 \tag{29}$$

$$\dot p_\theta = -p_r[\sin(\gamma_E - \theta) - v\sin(\gamma_P - \theta) + p_\theta[\cos(\gamma_E - \theta) - v\cos(\gamma_P - \theta)]/r, \qquad p_{\theta f} = 0 \tag{30}$$

$$\dot p_{\gamma E} = p_r\sin(\gamma_E - \theta) - p_\theta\cos(\gamma_E - \theta)/r, \quad p_{\gamma Ef} = 0 \tag{31}$$

$$\dot p_v = p_r\cos(\gamma_P - \theta) + p_\theta\sin(\gamma_P - \theta)/r - (\mathrm{d}H_P/\mathrm{d}v)v \qquad p_{vf} = 0 \tag{32}$$

$$\dot p_{\gamma P} = -p_r v\sin(\gamma_P - \theta) + p_\theta v\cos(\gamma_P - \theta)/r \qquad p_{\gamma Pf} = 0 \tag{33}$$

From the min-max principle, the optimal strategies on the barrier can be determined. For the evader

$$u_E^* = \mathrm{sign}(p_{\gamma E}), \qquad p_{\gamma E} \neq 0 \tag{34}$$

For a pursuer with a parabolic drag polar,

$$u_P^* = p_{\gamma P}/(2bp_v v) \tag{35a}$$

and for the pursuer with the nonlinear aerodynamic model,

$$\sin 2\alpha^* = \frac{-p_{\gamma P}}{\sqrt{(p_v v)^2 + (p_{\gamma P})^2}} \tag{35b}$$

$$\cos 2\alpha^* = \frac{-vp_v}{\sqrt{(p_v v)^2 + (p_{\gamma P})^2}} \tag{35c}$$

Fortunately, the adjoint equations of the present game [Eqs. (29-33)] can be integrated analytically, leading to explicit functions of the current and final state variables. This process, detailed in Appendix B, results [by selecting the value of $\mu$ in Eq. (29) as unity] in the following expressions:

$$p_r = \cos(\theta - \theta_f) \tag{36}$$

$$p_\theta = -r\sin(\theta - \theta_f) \tag{37}$$

$$p_{\gamma E} = -\sigma[\cos(\gamma_{Ef} - \theta_f) - \cos(\gamma_E - \theta_f)]\mathrm{sign}[\sin(\gamma_E - \theta_f)] \tag{38}$$

$$p_v = -\cos(\gamma_{Ef} - \theta_f)\tau/v \tag{39}$$

$$p_{\gamma P} = r\sin(\theta - \theta_f) - p_{\gamma E} \tag{40}$$

where

$$\tau = t_f - t' \tag{41}$$

is the normalized time to go. For small angles of attack

$$H^* = \cos(\gamma_{Ef} - \theta_f) - v\cos(\gamma_P - \theta_f) - ap_v v^2 + p_{\gamma P}{}^2/2bp_v = 0 \tag{42a}$$

and for the large-angle-of-attack model

$$H^* = \cos(\gamma_{Ef} - \theta_f) - v\cos(\gamma_P - \theta_f) - kp_v v^2 - v[(p_v v)^2 + p_{\gamma P}{}^2]^{1/2} = 0 \tag{42b}$$

The value of $\tau$ also can be obtained explicitly from Eqs. (38-42) as a function of the system state variables and their final values.

Equation (34) indicates that the possible existence of a singular control strategy is associated with $p_{\gamma E} = 0$ for some finite period of time. Substituting Eqs. (36) and (37) into Eq. (31) transforms it to

$$\dot p_{\gamma E} = \sin(\gamma_E - \theta_f); \qquad p_{\gamma Ef} = 0 \tag{43}$$

One can thus conclude that if $\gamma_{Ef} = \theta_f$ then

$$\dot p_{\gamma E}(t_f') = p_{\gamma Ef} = 0 \tag{44}$$

which leads to $p_{\gamma Ef}(t') \equiv 0$ for at least some finite period of time in the neighborhood of $t_f'$. The singular control strategy can be obtained differentiating once again $\dot p_{\gamma E}$ with respect to time,

$$\ddot p_{\gamma E} = \sigma\cos(\gamma_E - \theta_f)u_E \tag{45}$$

and equating $\ddot p_{\gamma E}$ to zero along the singular trajectory. It leads to the singular evader control,

$$u_E^s = 0 \tag{46}$$

implying that along the singular trajectory $\gamma_E^s = \gamma_{Ef} = \theta_f$. This singular trajectory is on a "universal surface" (US) of the evader. It reaches the target set, and its optimality is exhibited by attracting nearby barrier trajectories from both sides.[9] The pursuer strategy remains continuous on both sides of this US.

It is important to note that although a US in differential games has some similarity to a singular trajectory in optimal control problems, a clear distinction has to be made between them. In the game solution, the satisfaction of the sufficiency conditions, based on verifying that the US indeed attracts neighboring optimal trajectories, is of major importance. The well-known Kelley-Contensou test[10] of optimal control theory is only one of the necessary conditions implied by the verified optimality.

For all final conditions satisfying $\gamma_{Ef} \neq \theta_f$

$$u_E^* = -u_{EM} \operatorname{sign}[\sin(\gamma_E - \theta_f)] \tag{47}$$

It can thus be summarized that the evader's strategy is to turn toward the final line-of-sight direction. This strategy is identical to the one obtained in the "game of two cars."[3]

The optimal control strategy of the pursuer is obtained by substituting the expressions for $p_v v$ and $p_{\gamma p}$ from Eqs. (39) and (40) into Eqs. (35).

For the parabolic drag polar, one obtains

$$u_P^* = \frac{p_{\gamma E} - r \sin(\theta - \theta_f)}{2b \cos(\gamma_{Ef} - \theta_f)\tau} \tag{48a}$$

with $p_{\gamma E}$ given by Eq. (38). For the nonlinear aerodynamic model, also using Eq. (42b), the result is

$$\sin 2\alpha^* = \frac{p_{\gamma E} - r \sin(\theta - \theta_f)}{\left(\dfrac{1}{v} + k\tau\right) \cos(\gamma_{Ef} - \theta_f) - \cos(\gamma_p - \theta_f)} \tag{48b}$$

$$\cos 2\alpha^* = \frac{v_f \cos(\gamma_{Pf} - \theta_f)\tau}{\left(\dfrac{1}{v} + k\tau\right) \cos(\gamma_{Ef} - \theta_f) - \cos(\gamma_p - \theta_f)} \tag{48c}$$

Inspection of Eq. (48a) provides an interesting insight. The optimal strategy of the pursuer can be considered as being composed of two parts: a first part reacting to the evader's optimal maneuver (represented by $p_{\gamma E}$) and a second part compensating for the line-of-sight rotation. Moreover, the denominator in Eq. (48a) is proportional to the induced drag parameter of the missile, implying an optimal energy management.

For the high-angle-of-attack aerodynamic model [Eqs. (48b) and (48c)], there exists an interesting geometrical interpretation depicted in Fig. 2.

At the end of the game, the numerators and denominators in Eqs. (48) are all equal to zero. Thus, the final value of the pursuer's optimal control has to be obtained by the rule of l'Hopital,

$$\lim_{t' \to t_f'} p_{\gamma p}/(v p_v) = \lim_{t' \to t_f'} \dot{p}_{\gamma p}/\dot{\overline{(v p_v)}} \tag{49}$$

Using Eqs. (32) and (33), one obtains for small angles of attack

$$u_P^*(t_f) = -\tan(\gamma_{Pf} - \theta_f)/2b \tag{50a}$$

and for the high-angle-of-attack model

$$\tan 2\alpha^*(t_f) = -\tan(\gamma_{Pf} - \theta_f) \tag{50b}$$

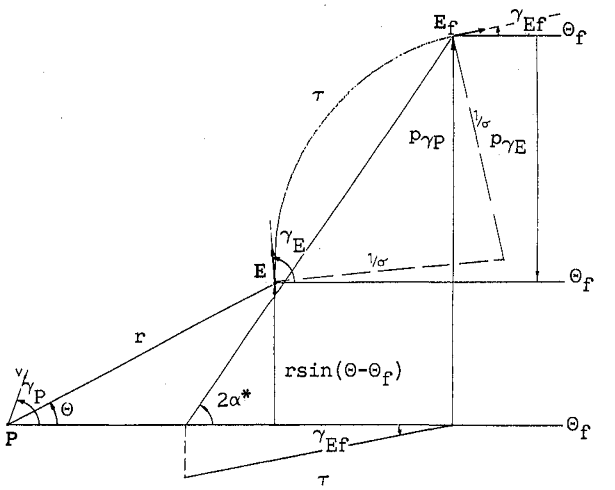


**Fig. 2 Pursuer evader controls geometric interpretation for the high-angle-of-attack model.**

Both expressions indicate that the pursuer's strategy is to turn toward the final line-of-sight direction, but this direction is never reached. This behavior is similar to the one observed in Ref. 4.

The only exception is $\gamma_{Pf} = \theta_f$. In this case $\dot{\gamma}_P(t') = 0$, and consequently $\gamma_P(t') = \theta_f$ throughout the entire pursuit. For this particular end condition Eq. (38) is simplified based on Eqs. (B7) and (B9) to

$$p_{\gamma E} = r \sin(\theta - \theta_f) \tag{51}$$

leading to

$$u_E^* = \operatorname{sign}[\sin(\theta - \theta_f)] \tag{52}$$

## IV. Barrier Construction

Since the optimal control strategies of the players are expressed by explicit functions of the state variables and their final values, the barrier trajectories can be constructed by a backward integration starting at the boundary of the useable part (BUP) of the target set.

For the barrier construction, the four-dimensional reduced space $r$, $\phi_E$, $v$, $\phi_P$ is employed. Without losing any generality, the final line of sight will be employed as the angular reference line, i.e., $\theta_f = 0$.

In the reduced space, the target set as well as the barrier are three-dimensional manifolds. The barrier supports itself in the two-dimensional BUP defined by

$$r = r_f, \qquad v_f = \cos\phi_{Ef}/\cos\phi_{Pf} \tag{53}$$

In the process of constructing barrier trajectories, $\phi_{Ef}$ and $\phi_{Pf}$ serve as two independent parameters. Integration of the trajectories stops at $v = v_0$. For this reason, it is convenient, since the game is autonomous, to use $v$ as the independent variable. In the computations presented in this paper, the aerodynamic model for small angles of attack in Eqs. (7) and (8), with parameters detailed in Table 1, was used.

The US of the evader discussed in the previous section is only one example of possible singularities. In effect, it is one of the easiest to discover because it generally terminates on the target set. It serves itself as the locus of attractive optimal trajectories. Every point on the US is a source of two optimal trajectories generated in retrotime by opposite control strategies of the respective player (in the present game the evader). Unlike most of the other singular surfaces in differential games, the adjoint vector is continuous on both sides of the US.

**Table 1 Parameters of the game, parabolic drag polar**

| Parameter | Symbol | Value |
|---|---|---|
| Minimum admissible turning radius of the pursuer | $R_{ref}$ | 1515.15 m |
| Evader velocity | $V_E$ | 300 m/s |
| Ratio of pursuer's minimum turning radius to that of the evader | $\sigma$ | 0.809 |
| Ratio of parasitic drag to maximum lift | $a$ | 0.0875 |
| Ratio of induced drag to lift at maximum lift coefficient | $b$ | 0.40 |

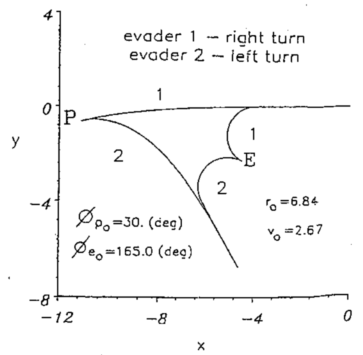


Fig. 3 Trajectory pair starting on the dispersal surface.

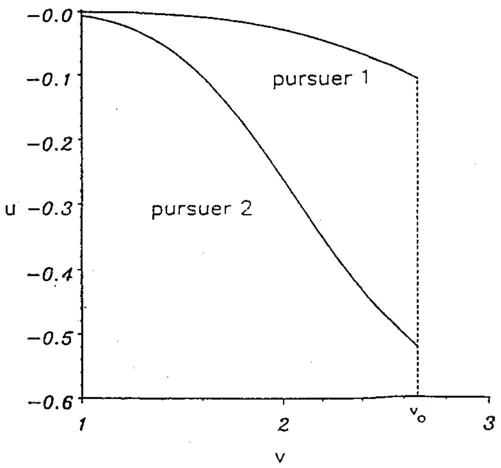


Fig. 4 Controls of the pursuer.

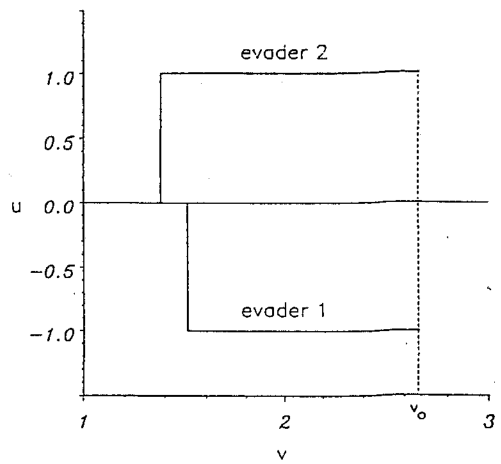


Fig. 5 Controls of the evader.

The most common example of a game singularity with a discontinuous adjoint vector is a "dispersal surface" (DS). Along such a surface one of the players (or both) has a choice to select different optimal strategies corresponding to different values of the respective adjoint variables. In the presently solved game, the existence of a DS on the barrier was discovered by the intersection of two families of barrier trajectories. Each point on this DS is associated with a pair of barrier trajectories terminating in different points of the BUP. An example of such a trajectory pair is depicted in Fig. 3.

As can be seen by comparing Figs. 4 and 5, both players have different controls along the intersecting trajectories. This indicates that on the DS both players have two different possible strategies. The evader has the choice between a left

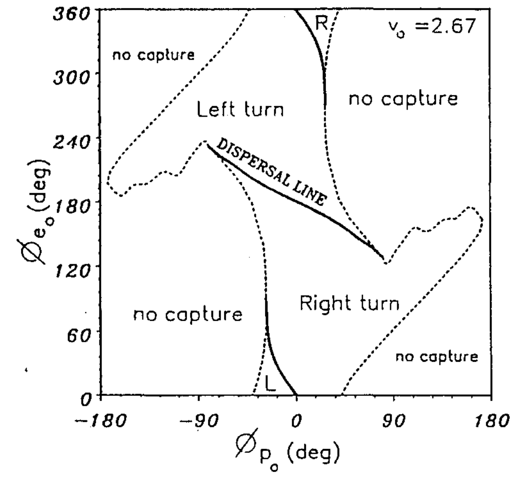


Fig. 6 Intersection of the capture zone with $v = v_0$ (projection on the $\phi_P - \phi_E$ plane, range contours omitted).

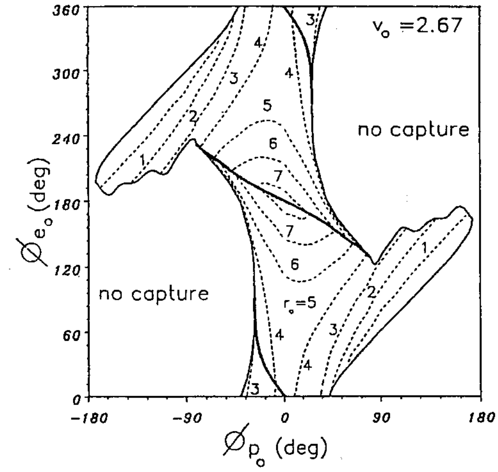


Fig. 7 Map of equal capture ranges at $v = v_0$ (projection on the $\phi_p - \phi_e$ plane).

turn or right turn, and the pursuer reacts to this choice accordingly.

As mentioned earlier, the barrier is a three-dimensional hypersurface in a four-dimensional state space ($r$, $\phi_E$, $v$, $\phi_P$) and therefore cannot be fully visualized as such. The intersection of this barrier with the hyperplane $v = v_0$ with $v_0$, a constant, is, however, a two-dimensional surface characterized by the set of points ($r_0$, $\phi_{E0}$, $\phi_{P0}$). For a given value of $v_0$, the "maximum capture range" $r_0$ is a function of the initial angular geometry represented by $\phi_{E0}$, $\phi_{P0}$.

In Figs. 6 and 7, the intersection of the barrier with the hyperplane $v_0 = 2.67$ ($V_{p0} = 800$ m/s) is displayed. Figure 6 is merely a qualitative one, showing, in the projection on the $\phi_{P0}$, $\phi_{E0}$ plane, the zone of capture and the respective optimal strategies of the evader. It also reveals a "dispersal line," the intersection of the DS with the initial velocity hyperplane. The intersection of the US with this hyperplane is also shown. It is the locus of the initial conditions for the optimal trajectories with singular evader control ($u_E^* = 0$). For sake of clarity, the contours of equal initial ranges on this hyperplane are depicted separately in Fig. 7. These two figures constitute together the description of the effective (no-escape) firing envelope of the missile for this given numerical example.

## V. Summary and Conclusions

In the present paper, the qualitative pursuit-evasion game between a coasting missile and a constant-speed aircraft in a horizontal plane is solved. The adjoint variables of the game are integrated analytically allowing us to express the optimal barrier strategies of the players as explicit functions of the current and final state variables.

The optimal strategy of the evader is a "hard" turn toward the direction of the final line of sight. If this direction is reached the evader continues in a straight line along the universal surface of the game. The pursuer's optimal strategy is also a turn toward the final line of sight with a turning rate, which is the sum of two components. The first part reacts to the evader's optimal maneuver, and the second part compensates for the line-of-sight rotation. This turning rate is inversely proportional to the induced drag parameter of the missile, implying an optimal energy management.

As a consequence of the explicit form of the barrier strategies, the optimal trajectories on the barrier can be obtained by retrograde integration of the state equations only, starting at the "boundary of the usable part" of the game. By using this process, the capture set of the game, equivalent to the effective (no-escape) firing envelope of the missile, can be determined.

As a part of the solution, two types of singular surfaces of the game were discovered: the universal surface and a dispersal surface. These surfaces separate the barrier of the game to regions of optimal left and right turns of the evader.

Since the control strategies found in the present study depend explicitly on the unknown final state variables, they cannot be directly implemented. Nevertheless, they can serve as the basis for a feedback guidance law synthesis, and furthermore, the results of the optimal game solution provide an excellent tool for comparing the performance of suboptimal control strategies.

## Appendix A: Nonlinear Aerodynamic Model

The aerodynamic normal and tangential forces $F_N$ and $F_T$ in body coordinates acting on $P$, functions of the angle of attack $\alpha$, are assumed to be of the form

$$F_N = \tfrac{1}{2}\rho V_P^2 S C_N \sin\alpha \tag{A1}$$

$$F_T = \tfrac{1}{2}\rho V_P^2 S C_T \cos\alpha \tag{A2}$$

where $C_N$ and $C_T$ are constant aerodynamic coefficients, $\rho$ is the air density, and $S$ an area. Gravitation effects are neglected.

Projecting forces along and normal to the pursuer velocity vector and rearranging

$$\dot V_P = -\rho S(C_N \sin^2\alpha + C_T \cos^2\alpha) V_P^2/2m \tag{A3}$$

$$\dot\gamma_P = \rho S(C_N - C_T) V_P \sin\alpha \cos\alpha/2m \tag{A4}$$

where $m$ is the pursuer's mass and a dot denotes the derivative with respect to time $t$.

Substituting $\sin\alpha$ and $\cos\alpha$ by their expressions in terms of $\sin 2\alpha$ and $\cos 2\alpha$ and rearranging, yields

$$\dot V_P = -c_1(k - \cos 2\alpha) V_P^2 \tag{A5}$$

$$\dot\gamma_P = c_1 V_P \sin 2\alpha \tag{A6}$$

where

$$c_1 = (C_N - C_T)\rho S/4m \tag{A7}$$

$$c_2 = (C_N + C_T)\rho S/4m \tag{A8}$$

$$k = c_2/c_1 > 1 \tag{A9}$$

For horizontal flight, $c_1$ and $c_2$ can be assumed constant.[5] The $1/c_1$ is the pursuer's minimum radius of curvature, as can be readily seen from Eq. (A6), a constant for horizontal flight. Equations (A5) and (A6) define the pursuer motion in a horizontal plane.

## Appendix B: Solution for the Adjoint Equations

This solution is based on the assumption that the adjoint vector, associated with the gradient of the barrier surface, is continuous. Substituting Eqs. (16) and (17) into Eqs. (29) and (30), one obtains

$$\dot p_r = p_\theta \dot\theta / r, \qquad p_{rf} = \mu > 0 \tag{B1}$$

$$\dot p_\theta = -p_r r \dot\theta + p_\theta \dot r / r, \qquad p_{\theta f} = 0 \tag{B2}$$

These two equations can be integrated to yield

$$p_r = \mu \cos(\theta - \theta_f) \tag{B3}$$

$$p_\theta = -\mu r \sin(\theta - \theta_f) \tag{B4}$$

where $\mu$ is the constant of integration and in particular can be normalized to 1 since the transversality condition (from where $\mu$ was derived) only fixes the direction and not the amplitude of the adjoint vector on the terminal surface.

Substituting Eqs. (B3) and (B4) into Eq. (26) and rearranging

$$\dot p_{\gamma E} = \sin(\gamma_E - \theta_f) \tag{B5}$$

Integrating Eq. (B5) and taking into account Eq. (17)

$$|p_{\gamma E}| = [\cos(\gamma_{Ef} - \theta_f) - \cos(\gamma_E - \theta_f)]/u_{EM} \tag{B6}$$

Substituting Eqs. (B3) and (B4) into Eq. (32) leads to

$$\dot p_{\gamma p} = -v \sin(\gamma_P - \theta_f) \tag{B7}$$

It can be readily shown that

$$\frac{\mathrm{d}(p_{\gamma E} + p_{\gamma P})}{\mathrm{d}t'} = \frac{\mathrm{d}[r \sin(\theta - \theta_f)]}{\mathrm{d}t'} \tag{B8}$$

which yields, since $p_{\gamma Ef} = p_{\gamma Pf} = 0$,

$$p_{\gamma p} = r \sin(\theta - \theta_f) - p_{\gamma E} \tag{B9}$$

Substituting Eqs. (B3), (B4), (B6), (33), and (34) into Eqs. (27) and (28a) and rearranging, leads for small angles of attack to

$$H^* = \cos(\gamma_{Ef} - \theta_f) - v \cos(\gamma_P - \theta_f)$$
$$- a p_v v^2 + p_{\gamma p}^2/2bp_v = 0 \tag{B10a}$$

whereas for the high-angle-of-attack model and with Eqs. (35b), (35c), and (28b) replacing Eqs. (35a) and (28a)

$$H^* = \cos(\gamma_{Ef} - \theta_f) - v \cos(\gamma_P - \theta_f)$$
$$- k p_v v^2 - v[(p_v v)^2 + p_{\gamma p}^2]^{1/2} = 0 \tag{B10b}$$

Multiplying Eq. (32) by $v$, Eq. (19) or (21) by $p_v$, and adding the result to the optimal Hamiltonian in Eq. (B10a) or (B10b), which is zero, one gets

$$\dot{\overline{v p_v}} = \cos(\gamma_{Ef} - \theta_f) \tag{B11}$$

Integrating Eq. (B11) backward leads to

$$v p_v = \cos(\gamma_{Ef} - \theta_f)\tau \tag{B12}$$

where

$$\tau = t'_f - t' \tag{B13}$$

This completes the integration of the adjoint variables as summarized in Eqs. (36–40).

## References


[1]Cockayne, E., "Plane Pursuit with Curvature Constraints," *SIAM Journal of Applied Mathematics*, Vol. 15, Nov. 1967, pp. 1511–1516.

[2]Rublein, G. T., "On Pursuit with Curvature Constraints," *SIAM Journal of Applied Mathematics*, Vol. 20, Jan. 1972, p. 37.

[3]Simakova, E. N., "The Quality Problem in Pursuit Games for Inertial Systems," *Automation and Remote Control*, Vol. 35, Nov. 1974, pp. 1716–1724.

[4]Prasad, U. R., Rajan, N., and Rao, N. J., "Planar Pursuit-Evasion with Variable Speeds, Part 1, Extremal Trajectory Maps," *Journal of Optimization Theory and Applications*, Vol. 33, No. 3, March 1981, pp. 401-418.

[5]Guelman, M., "The Attainability Domain of a Coasting Vehicle," *Journal of Optimization Theory and Applications*, Vol. 39, No. 3, March 1983, pp. 417–430.

[6]Guelman, M., "The Capture Region of a Coasting Pursuer," *Proceedings of the 24th Israeli Annual Conference on Aviation and Astronautics*, Technion, Israel, Feb. 1982, pp. 72-79.

[7]Shinar, J., "State Dependent Optimality of a Singular Subarc," *Automatica*, Vol. 24, March 1988, pp. 195–201.

[8]Blaquiere, A., Gerard, F., and Leitmann, G., *Qualitative and Quantitative Games*, Academic, New York, 1969.

[9]Isaacs, R., *Differential Games*, Wiley, New York, 1967.

[10]Kelley, H. J., Kopp, R. E., and Mayer, H. G., "Singular Extremals," *Topics in Optimization*, edited by G. Leitmann, Academic, New York, 1967.